# Estimation of ocean subsurface thermal structure from surface parameters: A neural network approach

M. M. Ali,[1] D. Swain,[1] and R. A. Weller[2]

Received 2 August 2004; accepted 24 September 2004; published 22 October 2004.

[1] Satellite remote sensing provides diverse and useful ocean surface observations. It is of interest to determine if such surface observations can be used to infer information about the vertical structure of the ocean's interior, like that of temperature profiles. Earlier studies used either sea surface temperature or dynamic height/sea surface height to infer the subsurface temperature profiles. In this study we have used neural network approach to estimate the temperature structure from sea surface temperature, sea surface height, wind stress, net radiation, and net heat flux, available from an Arabian Sea mooring from October 1994 to October 1995, deployed by the Woods Hole Oceanographic Institution. On the average, 50% of the estimations are within an error of ±0.5°C and 90% within ±1.0°C. The average RMS error between the estimated temperature profiles and in situ observations is 0.584°C with a depth-wise average correlation coefficient of 0.92. *INDEX TERMS:* 0930 Exploration Geophysics: Oceanic structures; 4572 Oceanography: Physical: Upper ocean processes; 0903 Exploration Geophysics: Computational methods, potential fields; 4263 Oceanography: General: Ocean prediction; 4594 Oceanography: Physical: Instruments and techniques. **Citation:** Ali, M. M., D. Swain, and R. A. Weller (2004), Estimation of ocean subsurface thermal structure from surface parameters: A neural network approach, *Geophys. Res. Lett.*, *31*, L20308, doi:10.1029/2004GL021192.

## 1. Introduction

[2] Satellite remote sensing provides diverse and useful ocean surface observations. Therefore, it is of value to determine the extent to which such surface observations can be used to develop information about the ocean's interior. Electromagnetic radiation does not penetrate deeply into the ocean waters because of which it is not possible to directly retrieve the subsurface information such as the vertical temperature profiles, one of the crucial parameters in physical oceanography. However, considering its importance and need in various applications, attempts have been made earlier to infer ocean subsurface thermal structure (OSTS) from surface parameters. Strategies for deriving subsurface information from surface parameters are based on either the combination of dynamical models and in situ observations [*Kao*, 1987; *Wunsch and Gaposchkin*, 1980] or purely on statistical relationships between the surface and the subsurface parameters. *Khedouri and Szczechowski* [1983] and *Fiedler* [1988] used purely statistical relationships between sea surface temperature (SST) and subsurface temperature profiles. *Chu et al.* [1997a, 1997b, 1999] developed a parametric model for analyzing observed temperature profiles based on a layered structure (mixed layer, thermocline, and deep layer). This model could successfully reproduce the historical temperature profiles of Yellow Sea and Beaufort/Chukchi Sea. Later *Chu et al.* [2000] used this model for determining OSTS from satellite SST observations, thus, establishing the inversion of the OSTS from satellite SST as a relation between SST and subsurface parameters such as mixed layer depth (MLD), thermocline bottom depth and thermocline temperature gradient. Altimeter derived sea surface height (SSH) is an indicator of vertical temperature structure [*Ali et al.*, 1998; *Cheney*, 1982; *Gopalan et al.*, 2000; *Gopalakrishna et al.*, 2003; *Khedouri and Szczechowski*, 1983]. *deWitt* [1987] used an empirical orthogonal function (EOF) analysis of OSTS and then developed relationships between dynamic height and the amplitudes of the first two vertical modes. These two modes could account for more than 95% of the temperature variance in each of the monthly data sets. *Carnes et al.* [1990] derived synthetic temperature profiles from Geosat SSH observations.

[3] All the earlier statistical approaches used only one parameter (e.g., SST, SSH or dynamic height) to synthesize the OSTS. However, the temperature structure depends upon many processes including surface heat exchange, wind-driven mixing, and advection. Hence, we believe that inclusion of surface parameters like wind speed, radiation/heat balance at the surface, SST and SSH/dynamic height that reflect these processes may prove to be more successful. In this paper, we have used a neural network approach to synthesize the OSTS using some of the surface parameters affecting the OSTS.

## 2. Data

[4] Woods Hole Oceanographic Institution had deployed a well-instrumented surface mooring in the central Arabian Sea during 16 October 1994–22 October 1995 in the middle of an array of four moorings deployed by Scripps Institution of Oceanography and the University of Washington [*Rudnick et al.*, 1997]. In the present analysis, we have used the observations from that mooring located at 15.5°N and 61.5°E. The surface element of this mooring was a 3 m discus buoy with two redundant sets of meteorological instruments, one vector-averaging wind recorder and one improved meteorological system. These instruments measured wind speed and direction at a height of about 3.2 m above the water level. They also measured air temperature, relative humidity, barometric pressure at a

[1]Oceanography Division, National Remote Sensing Agency, Balanagar, Hyderabad, India.
[2]Physical Oceanography Department, Woods Hole Oceanographic Institution, Woods Hole, Massachusetts, USA.


0094-8276/04/2004GL021192$05.00

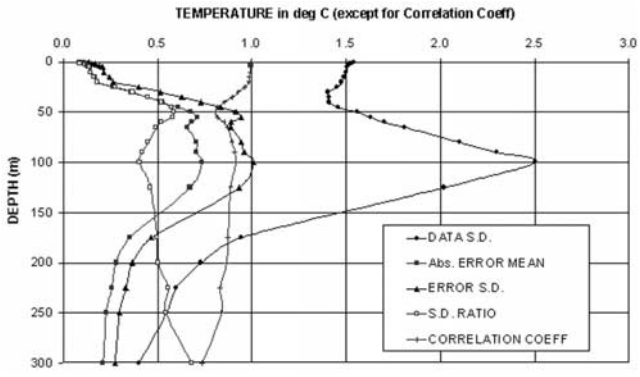


**Figure 1.** Neural network model summary statistics.

height of 2.5 m above the water line, incoming short wave and outgoing long wave radiation. The subsurface instrumentation consisted of vector measuring current meters, moored CT (conductivity, temperature sensors), temperature sensors and vector measuring current meters adapted to measure bio-optical parameters. The temperature measurements were made down to a depth of 3025 m and the salinity measurements down to 250 m.

[5] The net heat flux across the air-sea interface is computed from the surface buoy measurements. The details of these flux estimations and the accuracy of the measurements are described by *Weller et al.* [1998] and *Fischer* [1997]. The surface parameters used in this analysis are the net surface heat flux, net radiation, wind stress, SST, and the dynamic height. The dynamic height is estimated using the observations of temperature and salinity. At a few depths the salinity observations are not available all the time due to biofouling. In order to have uniformity in the computations of dynamic height, only those depths where the observations are available all the time were considered. Similarly, we have considered only those depths, where temperature observations were available throughout the study period. Thus, in total, we have considered 30 depths. We have discarded a few of the hourly observations for which some measurements were not available. Thus, out of the 8858 hourly observations we have considered 8306 measurements for the analysis. Though the temperature values are available down to 3025 m, we have considered only down to 300 m because the observations beyond 300 m are not regularly available. This is the only data set of both meteorological and oceanographic observations in the Indian Ocean with continuous time series of hourly frequency. Hence, we have selected this data set for the analyses, even though the observations are during 1994–1995.

## 3. Network Analysis

[6] Performing an artificial neural network (ANN) analysis requires three sets of data under the categories: Training, Verification (validation), and Prediction (testing). The data set marked for training is used to train the neural network. Verification cases are used to validate the model during training so that the model does not over-fit. The ANN stores the trained model and uses this model for predicting the outputs using the input parameters. The most popular algorithm for multi-layered networks is the back-propagation technique [*Miller and Emery*, 1997]. We have used the multi-layer perceptron model with a single hidden layer consisting of 14 hidden units, employing the back propagation algorithm for training [*Haykin*, 2002]. The independent parameters (inputs) for the network analysis are SST, dynamic height, wind stress, net radiation, and net heat flux. The dependent parameters are the temperatures at 30 depths. We have divided the entire data into even and odd dates. About 50% of the data with even dates are used for training and the remaining even dates data for verification. We have used all the data with odd dates (50% of the entire data set) for predicting the temperature profiles. Out of the total 8306 number of valid observations, we have used 2159 observations for training, 2080 for verification and 4067 for prediction. We have divided the data into odd and even dates so that the oceanographic conditions for training/verification and prediction remain same with the assumption that these conditions do not change significantly within a day. Among the five independent parameters dynamic height has the first rank followed by SST, net radiation, heat flux, and wind stress. The predicted values were compared with the in situ measurements and all the discussions and results in the subsequent sections refer to the comparison between the in situ and predicted values.

## 4. Results

[7] The data standard deviation (SD) (Figure 1) is maximum (~2.5°C) near 100 m depth and minimum (0.4°C) at deeper layers. Near the thermocline region, around 100 m, the temperature variations are large due to the changes in the MLD. Similarly, the SST variations are also large near the surface due to the variations in the radiation and fluxes and diurnal variability in near-surface stratification in light winds. Since the variation of temperature at deeper layers is negligible, the SD is also less. The absolute error mean and the SD of the error are very small in the surface layers indicating that temperatures closer to the surface can be estimated very accurately. Absolute errors are large near the thermocline region where seasonal variations are quite significant. The maximum absolute error mean and the SD error are of the order of 0.75°C and 1°C respectively. These errors are less in the deeper layers. Similarly, the SD ratio (the ratio between SD error and the data SD) is also less near the surface and in the deeper layers.

[8] Out of the 30 depths, where temperatures have been predicted, we have selected six depths for further analysis. All these depths are within the 50–125 m depth, where all the five statistical parameters described in Figure 1 show significant variations. Histograms of the errors in the model predicted temperatures are also prepared (figures not shown). At all these depths, the temperature could be estimated with an error limit of ±0.5°C in 50% of the cases, where as 95% of the estimations lie within ±1°C. 1–2°C errors account for only 5% of the total data set.

[9] We have computed the monthly RMS differences between the estimations and the actual observations at different depths (Figure 2). The monthly RMS differences down to 20 m and beyond 200 m depth are less than 0.5°C. Since the temperature profiles are estimated from the surface parameters, the errors are very less at the top 20 m layer. Similarly, the errors in the 200 m to 300 m range are

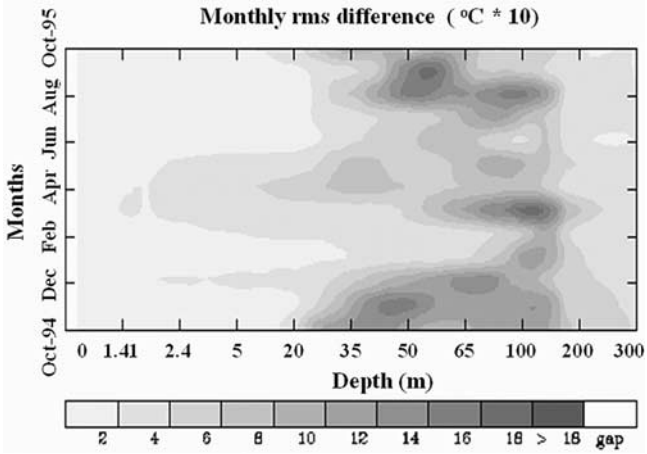


**Figure 2.** Monthly root mean square errors at different depths (x-axis is not to the scale).

also less as the temperatures at the deeper layers do not change significantly. Most of the errors are in the 35 m–150 m range where MLD has significant variations. The data SD is also high in this layer (Figure 1). *Carnes et al.* [1990] also observed large temperature error between the actual and synthetic temperatures near the core of the permanent thermocline. Largest RMS errors are present around March at 100 m depth. MLD, defined as the depth where the temperature gradient is more than 0.08°C/m [*Ali et al.*, 1987], has large variations at this depth. Other large RMS errors are observed during November 1994 and August/September 1995 at around 50 m. Incidentally, MLDs during these months are of the same range. Most of these errors are around 1°C with small patches of highest errors of the order of 1.8°C. However, the frequency of these high errors is quite less compared to the RMS errors of 0.5°C.

[10] Prediction of OSTS in the Arabian Sea is at some times of the year particularly challenging, and the prediction experiment has covered regimes characterized by different dynamics and upper ocean variability. The intermonsoon period of October and early November is characterized by light winds, net heat gain at the surface, and resulting diurnal variability in MLD [*Weller et al.*, 2002]. Strong diurnal variability, with MLDs ranging at times from close to 10 m during the day to close to 90 m at night, was observed at the Woods Hole Oceanographic Institution mooring during the northeast monsoon period of roughly mid-November through February. *Weller et al.* [2002] pointed to the mixed layer dynamics of this period being dominated by the surface buoyancy flux, with convective deepening of the mixed layer at night. The March–April intermonsoon showed MLD variability associated with short-lived changes in the sign of the surface heat flux and wind forcing events. Wind forcing dominated the dynamics in the southwest monsoon, and during that period the MLD showed little diurnal variability.

[11] The model is valid only if its RMS error is small and error SD is less than the in situ data SD. The SD ratio in the present study is less than 0.7 throughout indicating that the error SD is less than data SD, thus, validating the model used. The correlation coefficient (R) between model estimated and observed (in situ) profiles at all depths represents the second criterion for the model validity. The RMS error of all the estimated temperatures for all the depths is 0.584°C with a R value of 0.99. This reduces to 0.92 when we computed the R values first at each depth and then averaged over the 30 depths shown in Figure 1. *Chu et al.* [2000] used the inverse model in the South China Sea and estimated the temperature profiles with an average RMS error of 0.72°C and a R value of 0.79. However, they have estimated the temperature profiles over a larger area using the Master Observational Oceanographic Data Set (MOODS) for the South China Sea during May 1932–94.

[12] We have plotted the estimated temperature profiles along with the in situ observations for alternate months (for want of space) starting from November 1994 to September 1995 (Figure 3). Data of 0100 hrs (UTC) on 16th of every month have been used for this analysis. The vertical distribution of the estimated temperature agrees quite well with the in situ profiles. We have also analyzed the scatter plots for these twelve data sets (figures not shown). The regression equations and the corresponding coefficients of determination ($R^2$) values obtained from the scatter plots are also presented on each figure. In all the cases, the $R^2$ values are more than 0.97 with a slope of ~45°.

## 5. Summary and Conclusions

[13] The capability of the ANN approach to synthesize the OSTS from surface parameters like net surface heat flux, net radiation, SST, wind stress, and dynamic height is demonstrated in this paper. The observations of the Arabian Sea mooring located at 15.5°N and 61.5°E deployed by the Woods Hole Oceanographic Institution during October 1994 to October 1995 have been used for this analysis. The model estimated profiles were compared with the actual

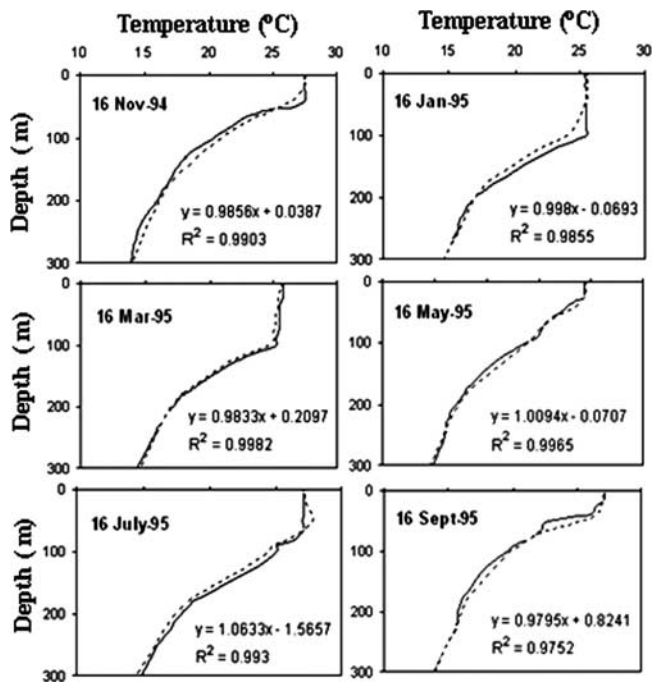


**Figure 3.** Comparison of in situ and predicted temperature profiles at different depths. Solid lines represent the in situ temperatures and dashed lines represent the estimated temperatures.

in situ profiles. They agreed quite well with the corresponding observed (in situ) profiles. About 50% of the estimated profiles lie within an error limit of ±0.5°C and 95% of the estimations, within ±1°C. 1–2°C errors account for only 5% of the total data set. The average RMS error of the model estimated profiles is 0.584°C, with a depth-wise average R value of 0.92.

[14] Thus, the ANN approach was found to be successful in estimating OSTS from surface parameters. To further strengthen and apply this model globally, it is necessary to test the validity of such an approach with widely varied sets of data from different regions and with better networks (models with more/optimum number of hidden layers and better training algorithms). This method may also be used in the estimation of salinity/density profiles, provided, more in situ measurements are available. Once accurate predictions of OSTS have been made, over a larger area, the estimated profiles can be used for the practical applications of acoustic propagation and MLD estimations.

[15] **Acknowledgments.** The authors express their gratitude to Dr. R. R. Navalgund, Director, National Remote Sensing Agency, Hyderabad, for his critical comments and suggestions. We had fruitful discussions with Mr. Asif Iqbal on the neural network analysis. The software provided by Prof. G. Mitchum to compute the dynamic heights is gratefully acknowledged. This work is carried out as a part of the Department of Ocean Development project. The authors are grateful to the referees for their constructive comments and suggestions.

## References

Ali, M. M., B. Simon, and P. S. Desai (1987), Inference of a vertical motion in the equatorial Indian Ocean using satellite data, *Oceanol. Acta.*, *6*, 71–76.

Ali, M. M., R. Sharma, and R. Cheney (1998), An atlas of the north Indian Ocean eddies from TOPEX altimeter derived sea surface heights, *ISRO-SAC-SP-69–98*, 6 pp., plate 39, Indian Space Res. Org., Bangalore.

Carnes, M. R., J. L. Mitchell, and P. W. deWitt (1990), Synthetic temperature profiles derived from Geosat altimetry: Comparison with air-dropped expendable bathythermograph profiles, *J. Geophys. Res.*, *95*, 17,979–17,992.

Cheney, R. E. (1982), Comparison data for Seasat altimetry in the western North Atlantic, *J. Geophys. Res.*, *87*, 3247–3253.

Chu, P. C., C. R. Fralick Jr., S. D. Haeger, and M. J. Carron (1997a), A parametric model for the Yellow Sea thermal variability, *J. Geophys. Res.*, *102*, 10,499–10,507.

Chu, P. C., H. C. Tseng, C. P. Chang, and J. M. Chen (1997b), South China Sea warm pool detected from the Navy's Master Oceanographic Observational Data Set (MOODS), *J. Geophys. Res.*, *102*, 15,761–15,771.

Chu, P. C., Q. Q. Wang, and R. H. Bourke (1999), A geometric model for the Beaufort/Chukchi Sea thermohaline structure, *J. Atmos. Oceanic Technol.*, *16*, 613–632.

Chu, P. C., C. Fan, and W. T. Liu (2000), Determination of vertical thermal structure from sea surface temperature, *J. Atmos. Oceanic Technol.*, *17*, 971–979.

deWitt, P. W. (1987), Modal decomposition of the monthly Gulf Stream/Kuroshio temperature fields, *NOO Tech. Rep. 298*, 40 pp., Nav. Oceanogr. Off., Stennis Space Center, Miss.

Fiedler, P. C. (1988), Surface manifestations of subsurface thermal structure in the California Current, *J. Geophys. Res.*, *93*, 4975–4983.

Fischer, A. S. (1997), Arabian Sea mixed layer deepening during the monsoon: Observations and dynamics, M.S. thesis, MIT/WHOI Joint Program in Oceanogr., Woods Hole, Mass.

Gopalakrishna, V. V., M. M. Ali, N. Araligidad, S. Shenoy, C. K. Shum, and Y. Yi (2003), An atlas of XBT thermal structures and TOPEX/Poseidon sea surface heights in the north Indian Ocean, *NIO-NRSA-SP-01–03*, Natl. Inst. of Oceanogr., Dona Paula, Goa, India.

Gopalan, A. K. S., V. V. Gopala Krishna, M. M. Ali, and R. Sharma (2000), Detection of Bay of Bengal eddies from TOPEX and in situ observations, *J. Mar. Res.*, *58*, 721–734.

Haykin, S. (2002), *Neural Networks: A Comprehensive Foundation*, 2nd ed., 842 pp., Pearson Education Asia, Singapore.

Kao, T. W. (1987), The Gulf Stream and its frontal structure: A quantitative representation, *J. Phys. Oceanogr.*, *17*, 123–133.

Khedouri, E., and C. Szczechowski (1983), Potential oceanographic applications of satellite altimetry for inferring subsurface thermal structure, *Proc. Conf. Mar. Technol. Soc.*, *1*, 274–280.

Miller, S. W., and W. J. Emery (1997), An automated neural network and cloud classifier for use over land and ocean surfaces, *J. Appl. Meteorol.*, *36*, 1346–1362.

Rudnick, D. L., R. A. Weller, C. C. Eriksen, T. Dickey, J. Marra, and C. Langdon (1997), One-year moored observations of the Arabian Sea, *EOS Trans. AGU*, *78*, 117, 120–121.

Weller, R. A., M. F. Baumgartner, S. A. Josey, A. S. Fischer, and J. C. Kindle (1998), Atmospheric forcing in the Arabian Sea during 1994–1995: Observations and comparisons with climatology and models, *Deep Sea Res., Part II*, *45*, 1961–1999.

Weller, R. A., A. S. Fischer, D. L. Rudnick, C. C. Eriksen, T. D. Dickey, J. Marra, C. Fox, and R. Leben (2002), Moored observations of upper-ocean response to the monsoons in the Arabian Sea during 1994–1995, *Deep Sea Res., Part II*, *49*, 2195–2230.

Wunsch, C., and E. M. Gaposchkin (1980), On using satellite altimetry to determine the general circulation of the oceans with application to geoid improvement, *Rev. Geophys.*, *18*, 725–745.

M. M. Ali and D. Swain, Oceanography Division, National Remote Sensing Agency, Balanagar, Hyderabad-500037, India. (mmali73@yahoo.com)

R. A. Weller, Physical Oceanography Department MS–29, Woods Hole Oceanographic Institution, Woods Hole, MA 02543, USA.